

1 **Title:** Leaf reflectance spectroscopy captures variation in carboxylation capacity across species,
2 canopy environment, and leaf age in lowland moist tropical forests

3
4 **Running Head:** Remote estimates of leaf carboxylation capacity

5
6 **Authors**

7 Jin Wu^{1*#}, Alistair Rogers¹, Loren P. Albert^{2,3}, Kim Ely¹, Neill Prohaska³, Brett T. Wolfe⁴,
8 Raimundo Cosme Oliveira Jr⁵, Scott R. Saleska³, and Shawn P. Serbin¹

9
10 **Affiliations**

11 [1] Environmental & Climate Sciences Department, Brookhaven National Laboratory, Upton,
12 New York, NY, 11973

13 [2] Institute at Brown for Environment and Society, Brown University, Providence, RI, 02912

14 [3] Department of Ecology and Evolutionary Biology, University of Arizona, Tucson, AZ, 85721

15 [4] Smithsonian Tropical Research Institute, Apartado 0843-03092, Balboa, Panama

16 [5] Embrapa Amazônia Oriental, Santarém PA 680200, Brazil

17
18 * Corresponding author

19 # Present address: School of Biological Sciences, University of Hong Kong, Pokfulam, Hong
20 Kong. Phone: (852) 22990655; Email: jinwu@hku.hk

21
22 **Key words:** vegetation spectroscopy, gas exchange, plant functional traits, seasonality, Earth
23 system models

24
25 **Type of Paper:** Original Research

26
27 **Words/Figures Record:**

28 **Word count:** summary (200 words); maintext and acknowledgements (6818 words)

29 **Figures:** 4 main figures + 3 supplementary figures

30 **Tables:** 2 supplementary tables

31

Author	Orchid Identifier
Jin Wu	0000-0001-8991-3970
Alistair Rogers	0000-0001-9262-7430
Loren P. Albert	0000-0002-9674-6071
Kim Ely	0000-0002-3915-001X
Neill Prohaska	no orchid Identifier
Brett T. Wolfe	0000-0001-7535-045X
Raimundo Cosme Oliveira Jr	no orchid Identifier
Scott R. Saleska	no orchid Identifier
Shawn P. Serbin	0000-0003-4136-8971

32

33 **Twitter:** @testgroup_bnl; @doctorjackpine; @kimberlite11; @albert_loren

34

35 **Summary**

- 36 • Understanding the pronounced seasonal and spatial variation in leaf carboxylation
37 capacity ($V_{c,max}$) is critical for determining terrestrial carbon cycling in tropical forests.
38 However, an efficient and scalable approach for predicting $V_{c,max}$ is still lacking.
- 39 • Here we tested the ability of leaf spectroscopy for rapid estimation of $V_{c,max}$. We
40 estimated $V_{c,max}$ using traditional gas exchange methods, and measured reflectance
41 spectra and leaf age in leaves sampled from tropical forests in Panama and Brazil. We
42 used these data to build a model to predict $V_{c,max}$ from leaf spectra.
- 43 • Our results demonstrated that leaf spectroscopy accurately predicts $V_{c,max}$ of mature
44 leaves in Panamanian tropical forests ($R^2=0.90$). However, this single-age model required
45 recalibration when applied to broader leaf demographic classes (i.e. immature leaves).
46 Combined use of spectroscopy models for $V_{c,max}$ and leaf age enabled construction of
47 the $V_{c,max}$ -age relationship solely from leaf spectra, which agreed with field observations.
48 This suggests that the spectroscopy technique can capture the seasonal variability
49 in $V_{c,max}$, assuming sufficient sampling across diverse species, leaf ages and canopy
50 environments.
- 51 • This finding will aid development of remote sensing approaches that can be used to
52 characterize $V_{c,max}$ in moist tropical forests and enable an efficient means to parameterize
53 and evaluate terrestrial biosphere models.

54 Introduction

55 Projecting the fate of terrestrial ecosystems under a changing climate requires knowledge
56 of plant physiology and ecology, and representation of that process knowledge in Earth system
57 models (ESMs). In particular, photosynthesis is a critical process to represent accurately. In the
58 most widely used model of photosynthesis, the rate of CO₂ assimilation is determined by the
59 maximum carboxylation rate of the enzyme Rubisco ($V_{c,max}$), the rate of RuBP regeneration
60 through electron transport, and in some models, the utilization of triose phosphates (Farquhar *et al.*,
61 1980; Sharkey *et al.*, 2007). The $V_{c,max25}$, which is $V_{c,max}$ standardized to a reference
62 temperature of 25°C (Bernacchi *et al.*, 2013), is a key parameter at the heart of many ESMs, and
63 variation in this parameter has repeatedly been shown to be the source of a large fraction of
64 overall model uncertainty (e.g. Bonan *et al.*, 2011; Rogers, 2014; Rogers *et al.*, 2017a; Walker *et al.*,
65 2017; Ricuitto *et al.*, 2018). Accurate and comprehensive observations of the biogeography,
66 ecology and overall distribution of $V_{c,max25}$ is thus a critical research need for improving
67 understanding and model predictions of photosynthesis at local, regional and global scales.

68 Most ESMs currently represent $V_{c,max25}$ with a single static value for each plant functional
69 type (Bonan *et al.*, 2011; Rogers, 2014). This assumption is most questionable for the tropical
70 forest biome where forests hold enormous plant functional diversity (Condit *et al.*, 2005; Steege
71 *et al.*, 2013; Asner *et al.*, 2014) that includes diversity in photosynthetic capacity (Norby *et al.*,
72 2017; Walker *et al.*, 2017). Furthermore, for a given species, $V_{c,max25}$ has been shown to vary
73 greatly with leaf development, growth temperature, and water and nutrient availability (Medlyn
74 *et al.*, 1999; Wilson *et al.*, 2001; Kenzo *et al.*, 2006; Kattge & Knorr, 2007; Ali *et al.*, 2015;
75 Norby *et al.*, 2017; Albert *et al.*, 2018; Kumarathunge *et al.*, 2019; Smith *et al.*, 2019). Recently
76 it was shown that the seasonality of photosynthesis in Amazonian evergreen forests, a ~ 4 Gt yr⁻¹
77 fluctuation in CO₂ assimilation (estimated using the envelop calculation approach to extend
78 existing site-level study in Amazon to the entire Amazon basin), is driven by the replacement of
79 old leaves that have a low $V_{c,max25}$ with recently matured leaves that have a higher $V_{c,max25}$ (Wu *et al.*,
80 2016; Albert *et al.*, 2018). These studies also demonstrated that it is critical to quantify leaf
81 age and couple this information with estimates of $V_{c,max25}$ to more accurately model leaf CO₂
82 assimilation by tropical forests. This result is likely also applicable to other vegetative biomes
83 that contain plants with long-lived leaves (e.g. needle-leaf evergreen) or with significant seasonal
84 variation (Wilson *et al.*, 2001; Han *et al.*, 2008; Muraoka *et al.*, 2010; Niinemets, 2016).

85 However, scaleable $V_{c,max25}$ data to enable this approach in models is lacking and tedious to
86 collect in the tropics, which is reflected in the very poor geographical coverage of tropical plants
87 in plant trait databases (Kattge *et al.*, 2011; Schimel *et al.*, 2015; Diaz *et al.*, 2016).

88 Typically, leaf-level $V_{c,max25}$ is estimated by fitting a model to a photosynthetic CO₂
89 response curve measured using gas exchange in a process that can take over forty-five minutes
90 for a single measurement (Long & Bernacchi, 2003). Although faster methods of estimating
91 $V_{c,max}$ have recently been described (DeKauwe *et al.*, 2016; Stinziano *et al.*, 2017), gas exchange
92 measurements remain challenging in natural systems such as tropical forests where many species
93 must be characterized at large scales. Canopy access presents an additional challenge in some
94 systems, including tropical forests where canopy height can exceed thirty meters, requiring
95 canopy cranes or tree climbing, which may be prohibitively time-consuming or expensive.
96 Moreover, reliably tracking leaf age, i.e. using the leaf tagging method with intensive *in-situ*
97 revisits and surveys (Reich *et al.*, 2004; Wu *et al.*, 2017), coupled with leaf gas exchange
98 measurements, adds another level of difficulty. This challenge is particularly acute for moist
99 tropical forests in which periods of new leaf production can last from a week up to a year, and
100 different tree species have distinct and often irregular new leaf production patterns both in their
101 timing and amplitude (Reich *et al.*, 2004; Lopes *et al.*, 2016; Xu *et al.*, 2017). Within this
102 context, researchers require methods that allow rapid estimation of $V_{c,max25}$ and leaf age that can
103 be applied to tall trees in natural systems, including remote tropical forests.

104 Recent advances in vegetation spectroscopy offer a promising solution given that this
105 approach tightly connects leaf optical properties with their chemical composition, cell structure
106 and physiological properties (Curran, 1989; Elvidge, 1990; Kokaly *et al.*, 2009). As such,
107 spectroscopy has been receiving increasing attention from a broader science community,
108 including those from plant ecophysiology, functional trait ecology, and evolution (Serbin *et al.*,
109 2012; Asner *et al.*, 2016; Schneider *et al.*, 2017; Schweiger *et al.*, 2018). For example, recent
110 studies suggest that leaf $V_{c,max}$ can be estimated accurately and rapidly based on leaf reflectance
111 spectra (e.g. Doughty *et al.*, 2011; Serbin *et al.*, 2012; Ainsworth *et al.*, 2014; Barnes *et al.*, 2017;
112 Dechant *et al.*, 2017; Yendrek *et al.*, 2017; Silva-Perez *et al.*, 2018). In addition, two recent
113 studies have also shown that leaf spectroscopy provides an accurate, rapid means to assess leaf
114 age at both individual and community scales (Chavana-Bryant *et al.*, 2017; Wu *et al.*, 2017).
115 Furthermore, some studies also suggest that it is possible that spectroscopy-based models of leaf

116 $V_{c,max25}$ and age could be extended to the canopy scale by leveraging imaging spectroscopy
117 instrumentation on tower, unmanned aerial systems, and manned airborne platforms (Serbin *et*
118 *al.*, 2015; De Moura *et al.*, 2017). These developments highlight the potential to map changes in
119 $V_{c,max25}$ and leaf age over unprecedented spatial and temporal scales. However, the ability of
120 spectra to predict the variability in $V_{c,max25}$ across these multiple axes of variation (i.e. species,
121 canopy position, leaf age, and forest sites) has not been tested, and a spectroscopy-based
122 approach that can account for variation in both leaf age and $V_{c,max25}$ has not been developed.

123 In this study we collected leaf gas exchange, reflectance spectroscopy and leaf age data
124 from three lowland moist tropical forests. Our goal was to develop a single spectroscopic
125 approach capable of capturing the variation in $V_{c,max25}$ among leaves of different ages from a
126 range of species and canopy environments (i.e. variation in canopy height and sunlit and shaded
127 environments) in lowland moist tropical forests. We asked two main questions: (1) Can the
128 spectra- $V_{c,max25}$ relationship for mature leaves also be applied to leaves of other leaf demographic
129 classes (e.g. immature leaves), and if not, can a new spectra-based model of $V_{c,max25}$ be developed
130 that performs well across all leaf ages? (2) Can leaf spectra information alone enable accurate
131 estimation of the developmental trajectories of $V_{c,max25}$, i.e. the $V_{c,max25}$ –leaf age relationship? By
132 answering these questions, we hope to understand if the spectroscopy approach can be used to
133 capture the $V_{c,max25}$ variability in moist tropical forests, thereby accelerating current capacity to
134 parameterize ESMs for improved projection of terrestrial carbon and water fluxes in the context
135 of a changing climate.

136

137 **Materials and Methods**

138 *Site descriptions*

139 This study used data collected from three lowland seasonal moist tropical forests,
140 including two crane sites in the Republic of Panama and one site in Brazil. The two sites in
141 Panama include a seasonally dry forest in the Parque Natural Metropolitano (PNM; 8.9950° N,
142 79.5431° W) near Panama City and a wet evergreen forest in the San Lorenzo Protected Area
143 (SLZ; 9.2810° N, 79.9745° W), Colon Province. Both sites are dominated by clay soil (Turner &
144 Romero, 2009). Mean annual air temperature at both sites is 26 °C (1998–2015), and mean
145 annual precipitation is 1826 mm yr⁻¹ and 3286 mm yr⁻¹ for PNM and SLZ, respectively, with a 4-
146 month-long dry season (precipitation < 100 mm per month) from January to April each year. At

147 each site, the Smithsonian Tropical Research Institute maintains a canopy-access crane that
148 enables access throughout the canopy of these forests. The site in Brazil (2.8500° S, 54.9667° W)
149 is located around the K67 eddy covariance site in Tapajos National Forest, near Santarem, Para,
150 Brazil. Part of the Brazilian Large Scale Biosphere-Atmosphere Experiment in Amazonia (LBA;
151 Davidson *et al.*, 2012), this site sits on a well-drained clay-soil plateau. Multiple-year (2002–
152 2005) mean annual air temperature is 26 °C (Hutyra *et al.*, 2007). Mean annual precipitation
153 (1998–2013) is 2022 mm yr⁻¹ with a 5-month-long dry season from mid-July to mid-December
154 each year. Single rope access techniques were used to climb into and access individual crowns of
155 canopy trees (Albert *et al.*, 2018). For details about forest composition and structure of the sites
156 in Panama see Wright *et al* (2003), and of the site in Brazil see Rice *et al* (2004). For information
157 about soil fertility of the sites in Panama see Turner & Romero (2009), and of the site in Brazil
158 see Nepstad *et al* (2002).

159

160 *Plant materials*

161 Sixteen canopy tree species from the two sites in Panama ($n=8$ for SLZ and $n=8$ for
162 PNM) and five canopy tree species from the Brazilian site were selected for intensive field
163 measurements of leaf gas exchange, reflectance spectra and traits (i.e. leaf mass per area, LMA;
164 Table S1). Sampled leaves were classified into two main age classes: immature leaves (<2
165 months; corresponding to the leaves from emergence up to fully-expanded, but not fully green,
166 thickened, or physiologically matured) or mature leaves (≥ 2 months old), following the similar
167 age categories as presented in Coley (1983), Wu *et al* (2016), and Albert *et al* (2018). This
168 classification of leaf age is very similar to the three-age-category (young, mature and old) used in
169 Wu *et al* (2016), except that we grouped mature and old age classes together into a single age
170 class, mature. The reason of doing this is because we didn't track leaf age as frequently in
171 Panama as that in Brazil (Wu *et al.*, 2017), and therefore lacked the resolution to differentiate
172 three age classes. Field measurements in Panama were conducted in the 2016 and 2017 dry
173 seasons on sunlit upper canopy foliage. In the 2016 field campaigns in mid-February and mid-
174 April we sampled the dominant leaf class(es) from eight trees at each site. In February 2017 the
175 measurements included both age classes if present within the top meter of a sunlit branch from
176 four canopy tree species at the SLZ site (Table S1). Field measurements of canopy trees in
177 Brazil, including leaves of both age classes from sunlit and shaded branches, were conducted

178 during the 2012 dry season field campaign from mid-August until early-December and a 2013
179 dry season campaign in August, using single-rope access techniques. For more details on
180 surveyed tree species, please refer to our Table S1 & Albert *et al* (2018).

181

182 *Field measurements*

183 (1) Leaf gas exchange. We used six portable gas exchange systems in Panama and two in
184 Brazil (LI-6400XT, Li-COR Inc., Lincoln, NE, USA). Measurements of the response of net
185 assimilation rate (A) to intra-cellular CO₂ concentration (C_i), commonly known as A - C_i response
186 curves, were conducted on leaves from cut branches. In Panama, all branches were sampled
187 before dawn using the canopy cranes. We took steps to avoid inducing xylem embolism when
188 collecting branches, and when it was possible, the initial cut was made under water by bending
189 the branch section into a bucket filled with water. Otherwise, the initial cut was made in the air
190 and then a second cut was made underwater approximately 1 meter from the initial cut. In all
191 cases, several cuts were made sequentially closer to the branch tip to relax xylem tension,
192 following the protocol as described by Sperry (2013). Samples were stored in individual buckets
193 and kept in deep shade until used for measurements, which was normally within four hours after
194 harvesting. Measurements of A - C_i curves closely followed Rogers *et al* (2017b), with the
195 reference CO₂ concentration controlled as follows: 400, 325, 250, 175, 100, 65, 40, 400, 400,
196 400, 475, 575, 675, 800, 1000, 1400 and 1800 $\mu\text{mol mol}^{-1}$, while holding leaves at 31 ± 2 °C and
197 $83\pm 5\%$ relative humidity under saturated light condition (i.e. 2000 $\mu\text{mol m}^{-2} \text{s}^{-1}$). In Brazil,
198 branch samples were collected via tree climbing, and gently lowered to the ground with ropes in
199 the morning, and re-cut under water within 15 minutes. Samples were stored in individual
200 buckets and kept in deep shade until used for measurements (typically within four hours after
201 harvesting). Full details of leaf gas exchange measurements from Brazil are in Albert *et al*
202 (2018). In brief, the protocol was similar as that was described above except that in Brazil, the
203 reference CO₂ concentration was controlled as follows: 400, 100, 50, 100, 150, 250, 350, 550,
204 750 $\mu\text{mol mol}^{-1}$, and then increased by increments of between 200 to 500 to reach saturation at
205 around 2000, and leaf temperature was controlled at 31 ± 2 °C and chamber humidity was
206 controlled at $46\pm 11\%$.

207 Prior to curve fitting, quality control procedures for gas exchange measurements from all
208 sites excluded values associated with instrument error and other known artifacts, such as

209 spurious logs and data where leaks were clearly apparent, as described in Rogers *et al* (2017b)
210 and Albert *et al* (2018). Finally, apparent maximum carboxylation capacity standardized to a
211 reference temperature of 25°C ($V_{c,max25}$) was estimated using the kinetic constants and
212 temperature response functions presented by Bernacchi *et al* (2013) as described by Rogers *et al*
213 (2017b). A total of 186 leaves with estimated $V_{c,max25}$ in Panama and 81 leaves in Brazil were
214 used in this study, with species-specific mean and standard deviation summarized in Table S1.

215 (2) Leaf spectra. Following leaf gas exchange measurements, we kept the branches in
216 water and within two hours harvested the leaf and immediately measured leaf reflectance spectra
217 and fresh mass. Leaf reflectance at the Panamanian sites was measured using a Spectra Vista
218 Corporation (SVC) HR-1024i (SVC, Poughkeepsie, NY, USA; spectral range: 350–2500nm;
219 spectral resolution: 3.5 nm at 700nm, 9.5 nm at 1500 nm, and 6.5 nm at 2100 nm) together with
220 the SVC LC-RP-Pro foreoptic. Similarly, leaf reflectance of Brazilian plants was measured using
221 a FieldSpec® Pro spectrometer (Analytical Spectra Devices, ASD, Boulder, CO, USA; spectral
222 range: 350–2500nm; spectral resolution: 3 nm at 700nm, 10 nm at 1400 nm, and 10 nm at 2100
223 nm) together with a ASD leaf clip attached to a plant probe assembly. In both cases, the
224 reflectance probes contained internal, calibrated light sources to illuminate the samples during
225 spectral collection. The leaf probe was used together with a black background for leaf reflectance
226 measurements. To avoid the excessive heat loads while ensuring the reliable spectral collection
227 we set the ASD integration time to 100 milliseconds per scan and each collected spectra was an
228 average of 10 scans, while with the SVC we used a 1 second collection time and used the
229 spectrometer's automatic integration optimization. This approach matches that of Serbin *et al*
230 (2012), which originally highlighted the concerns of the excessive heat loads on the data quality
231 of leaf spectra collected. For each leaf, reflectance spectra were measured on 1–6 different parts
232 of the leaf adaxial surface depending on leaf size, and then averaged to determine the mean
233 optical properties across all wavelengths.

234 (3) Leaf traits. Leaf mass per area (LMA; g m^{-2}) was also measured to assess the diversity
235 of plant species that we sampled in terms of the LMA trait space. In Panama, we sampled a
236 known leaf area using cork borers. The samples were dried to constant mass at 70°C. We then
237 determined dry mass with a precision balance (Fisher Science Education, Model SLF303,
238 Hanover Park, IL, USA) to calculate LMA. In Brazil, LMA was derived from area (using a

239 Canon LiDE 120 scanner) and dry weight (also using a precision balance from Fisher Science
240 Education, Model SLF303, Hanover Park, IL, USA) oven-dried at 60°C for over 72 hours.

241 (4) Leaf age. In Brazil, in field campaigns conducted in August–September 2013,
242 November 2013, March 2014 and July–August 2014, we selected seven trees of different species
243 (see Table 1 in Wu *et al.*, 2017) for precise *in-situ* leaf age monitoring. Leaf age monitoring was
244 carried out by using metal tags and *in-situ* photo documentation (e.g. Fig. S1 in Wu *et al.*, 2017).
245 Monitoring began in August–September 2013, when most sampled trees were flushing new
246 leaves, and was continued periodically throughout the annual cycle. Through this age-tagging
247 technique, we accurately tracked leaf age from leaf emergence at budburst (0 day) up to ~400
248 days old. From those leaves with accurate leaf age monitoring, we then sampled a total of 759
249 leaves covering the entire annual cycle, and measured leaf reflectance spectra using the same
250 ASD FieldSpec® Pro spectrometer as described above. These leaves were then used for the
251 development of the community-level spectra-age model (Wu *et al.*, 2017) and briefly
252 summarized below. Among these seven trees surveyed for both leaf age monitoring and leaf
253 reflectance measurements, four were the same canopy trees (including leaf samples from both
254 sunlit and shaded microenvironments) from which we made gas exchange measurements as
255 described above (also see Table S1).

256 In addition to the above-mentioned accurate leaf age monitoring, we also took RGB
257 photos for all leaves used for leaf reflectance measurements in both Panama and Brazil. These
258 RGB photos together with other related information, e.g. visual assessment of color, size and
259 rigidity of the leaves, and relative positions and bud scars (when present) within a 1-meter
260 branch length, were then used to classify these leaves into two different age categories: immature
261 and mature leaves.

262 (5) Spectra- $V_{c,max25}$ analysis. For all field-based spectral and gas exchange measurements
263 in Panama and Brazil, only the plant species with both leaf reflectance spectra and $V_{c,max25}$ were
264 selected (which excluded 25 measurements in Panama and 12 measurements in Brazil with only
265 leaf gas exchange). Finally, we performed a filtering of outliers of combined spectra- $V_{c,max25}$
266 datasets (which removed ~5% of data). The outlier detection method implemented here was
267 originally used in Wu *et al.* (2017), which adapted an outlier detection module from “libPLS”
268 (accessed at <http://www.libpls.net/>), using the Monte-Carlo sampling method (Xu & Liang,
269 2001) for automatic outlier detection. After the data filtering, the Panamanian dataset had $n=151$

270 measurements, including 110 mature leaves from all 16 species and 41 immature leaves from 9
271 of the 16 species, which accounts for 94% of all measurements with both spectral and leaf gas
272 exchange in Panama. Brazilian dataset had $n=65$ measurements, including 44 mature leaves and
273 21 immature leaves from all 5 species, which accounts for 94% of all measurements with both
274 spectral and leaf gas exchange in Brazil.

275 All the data sources associated with this study including gas exchange data, leaf spectral
276 data, leaf trait, and leaf age information were summarized in Table S2.

277

278 *Partial least-squares regression (PLSR) modeling of spectra- $V_{c,max25}$ and spectra-age*

279 To relate the variability in $V_{c,max25}$ across tree species, leaf age, canopy position, and
280 forest sites with the variability in leaf reflectance spectra and to infer leaf age from leaf
281 reflectance spectra, we utilized a PLSR modeling approach (Geladi & Kowalski, 1986; Wolter *et*
282 *al.*, 2008) using the “plsregress” function in Matlab (Mathworks, Natick, MA, USA) as described
283 in De Jong (1993) and Rosipal & Kramer (2006). PLSR is a commonly-used approach in
284 spectroscopy and chemometric analyses given its ability to handle high predictor collinearity and
285 a large number of predictor variables that may exceed the number of observations. PLSR
286 accounts for these challenges by reducing the number of predictor variables down to relatively
287 few, orthogonal latent variables, each composed of a weighted sum of the original variables
288 (Geladi & Kowalski, 1986; Wolter *et al.*, 2008). Moreover, PLSR accounts for measurement
289 error in the predictor variables (i.e. leaf hyperspectral reflectance).

290 Our PLSR model development has been described previously (Wu *et al.*, 2017) and is
291 briefly summarized here. We first applied a square root transformation to the $V_{c,max25}$ data and
292 leaf age data to reduce the right skewness distribution of the original data (e.g. Figs. S1a,b and
293 S2a,b) and satisfy the normal distribution assumption of PLSR analysis. We then performed a
294 one-time, random, stratified separation of the full dataset into calibration (two thirds) and
295 independent validation (one third) subsets; stratification insured that each subset included leaf
296 samples of each age category, of each species, and (when appropriate) of each canopy position.
297 Next, we randomly selected 70% of the calibration data subset, and fit the PLSR model of
298 spectra- $V_{c,max25}$, with this random selection, repeating this 100 times and for each permutation
299 applying the model to predict the corresponding independent 30% of the calibration data. To
300 avoid the potential to over-fit the spectra-based calibration model, we optimized the number of

301 PLSR latent variables by choosing the number of latent variables that minimized the root mean
302 square error (RMSE) from predicting the remaining 30% of the calibration data over the 100
303 permutations (Chen *et al.*, 2004; e.g. Fig. S1c). Meanwhile, we also determined the mean and
304 standard deviation of the distribution of PLSR coefficients generated by the 100 PLSR fits
305 corresponding to the optimal number of latent variables, which were used in the final spectra-
306 $V_{c,max25}$ model (e.g. Fig. S1d).

307 Finally, we quantified the performance of this spectra- $V_{c,max25}$ model using the
308 independent validation dataset. We used three main evaluation metrics: the coefficients of
309 determination (R^2), RMSE, and the regression bias. All model results presented in this study are
310 shown in the original $V_{c,max25}$ units rather than the square root transformed unit that is the initial
311 output of the PLSR model. The same spectral analytical approach was applied to the Brazilian
312 spectra-age dataset to derive the community-level spectra-age model (Fig. S2 and Wu *et al.*,
313 2017). All of the code used for model development and data analysis were developed in Matlab
314 (Mathworks, Natick, MA, USA).

315

316 *Generalizability of spectra- $V_{c,max25}$ relationship*

317 We explored whether the spectra- $V_{c,max25}$ relationship can be generalized across species,
318 leaf age and canopy environment through two tests. In the first test, we developed a spectra-
319 based PLSR model using two-thirds of the Panamanian data for mature leaves to train the model
320 (including all 16 species). We then applied this model to the remaining Panamanian dataset of
321 mature leaves, as well as to the independent validation dataset of Panamanian immature leaves,
322 and Brazilian mature and immature leaves. Through this test, it would enable us to assess
323 whether the spectra- $V_{c,max25}$ relationship of mature leaves can also be applied to leaves of
324 immature age class or leaves of a different forest site in Brazil. In the second test, we developed
325 a new spectra-based model in which all our datasets (including two-thirds of all leaves from both
326 Panama and Brazil) were used to train the model. Model performance was evaluated using the
327 remaining, independent datasets, which are the same as that were used in the first test. Through
328 this test, it would enable us to assess whether a single spectra- $V_{c,max25}$ relationship can be applied
329 to leaves of both leaf age classes and different forest sites.

330

331 *Spectral-based seasonal variability in $V_{c,max25}$, or $V_{c,max25}$ -age relationship, using a combination*
332 *of spectral models of $V_{c,max25}$ and leaf age*

333 With the developed spectra- $V_{c,max25}$ model and spectra-age model as described above, we
334 then used these two models in combination to explore whether leaf spectra information alone can
335 be used to reconstruct the life history variability in leaf $V_{c,max25}$ for tropical trees. The spectra-age
336 dataset in Brazil were used for this test, as the dataset covered the leaf spectra throughout their
337 life cycles (Wu *et al.*, 2017) while having some ground truth of $V_{c,max25}$ derived from gas
338 exchange measurements (Albert *et al.*, 2018). These two models are both at the community level
339 and their model regression coefficients are respectively shown in Figs. S1d and S2d. The models
340 were driven by the input of leaf spectral reflectance only but can predict leaf $V_{c,max25}$ and leaf age
341 respectively (see the provided sample Matlab script). By combining the model output of $V_{c,max25}$
342 and age together, the spectroscopy approach was thus used to estimate the $V_{c,max25}$ -age
343 relationship, or the life history variability in leaf $V_{c,max25}$ with leaf age.

344

345 **Results**

346 As shown in Fig. 1 and Table S1, we found large variability in leaf $V_{c,max25}$ for the
347 surveyed 21 tropical trees from three tropical forest sites: field-measured $V_{c,max25}$ ranged from 7-
348 102 $\mu\text{mol CO}_2 \text{ m}^{-2} \text{ s}^{-1}$. These surveyed trees also spanned a very large variation in leaf
349 morphology, as shown in the observed LMA trait space (i.e. 70-213 g m^{-2}). We also found that
350 the variation in $V_{c,max25}$ is attributable to species (Fig. 1a and Table S1), leaf age (mature vs.
351 immature; Fig. 1a), canopy environment (sunlit vs. shaded; Fig. 1a), and also forest sites (Fig.
352 1b). The large intra-specific variation in $V_{c,max25}$ is primarily associated with leaf age, and the
353 large inter-specific variation in $V_{c,max25}$ is attributable to both species difference but also the
354 forest sites. Such large variation in $V_{c,max25}$, especially the variation with leaf age, will make the
355 traditional approaches for measuring this diversity challenging due to the requirement for lots of
356 measurements.

357 We examined our first question of whether the spectroscopy approach can be an efficient,
358 alternative means to help estimate $V_{c,max25}$ across species, leaf age, canopy environment and
359 forest sites through the two tests (see Methods above). In the first test, we found that the model
360 based solely on Panamanian mature leaves was able to predict the field-observed $V_{c,max25}$ of
361 independent Panamanian mature leaves with very high accuracy ($R^2=0.90$; $\text{RMSE}=5.9 \mu\text{mol}$

362 $\text{CO}_2 \text{ m}^{-2} \text{ s}^{-1}$; $n=36$ leaves; Fig. 2a), suggesting a tight covariation in the spectra- $V_{c,max25}$
363 relationship for Panamanian forests across a diverse range of tree species, canopy heights and
364 leaf traits (Table S1). However, this model did not perform as well when applied to a dataset of
365 independent, Panamanian immature leaves from a subset of the same trees ($n=9$ species; Table
366 S1), with the model fit having a marked deviation from the 1:1 line (between modeled and
367 observed $V_{c,max25}$) and displaying poor predictive ability ($R^2=0.02$; $\text{RMSE}=20.7 \mu\text{mol CO}_2 \text{ m}^{-2} \text{ s}^{-1}$;
368 $n=14$ leaves; Fig. 2b). When the model of Panamanian mature leaves was applied to
369 independent, Brazilian mature and immature leaves the model performance was also poor
370 ($R^2=0.23$; $\text{RMSE}=38.8 \mu\text{mol CO}_2 \text{ m}^{-2} \text{ s}^{-1}$; $n=22$ leaves; Fig. 2c). This showed that the model
371 developed from Panamanian mature leaves could neither be directly applied to immature leaves
372 of the same trees nor the leaves sampled from other tropical forests without marked reduction in
373 predictive power (Fig. 2d).

374 In the second test, we found that the new model trained on the data from all species, leaf
375 ages, canopy environment, and forest sites performed dramatically better across the whole range
376 of leaf types—immature leaves in Panama ($R^2=0.89$; $\text{RMSE}=3.9 \mu\text{mol CO}_2 \text{ m}^{-2} \text{ s}^{-1}$; $n=14$ leaves;
377 Figs. 3 and S3a) and all leaf ages from Brazil ($R^2=0.68$; $\text{RMSE}=5.9 \mu\text{mol CO}_2 \text{ m}^{-2} \text{ s}^{-1}$; $n=22$
378 leaves; Figs. 3 and S3b)—at the cost of only slightly lower prediction of mature Panamanian
379 leaves ($R^2=0.86$; $\text{RMSE}=7.7 \mu\text{mol CO}_2 \text{ m}^{-2} \text{ s}^{-1}$; $n=36$ leaves; Figs. 3 and S3c). In addition,
380 compared with our initial model of Panamanian mature leaves (Fig. 2, first test), the new model
381 (Fig. 3, second test) also significantly reduced the uncertainty in model predicted $V_{c,max25}$, as
382 indicated by the horizontal error bars shown in Figs. 2 and 3. This analysis demonstrated that
383 with sufficient leaf samples to train the spectra- $V_{c,max25}$ relationship over the full trait space, a
384 general spectra-based $V_{c,max25}$ model can be derived across species, leaf age, canopy
385 environment, and forest sites.

386 We next examined our second question: whether the spectroscopy approach alone is
387 sufficient to simulate the life history trajectories of $V_{c,max25}$, or the $V_{c,max25}$ -age relationship. To do
388 this, we applied two models (i.e. the community-level spectra- $V_{c,max25}$ model and spectra-age
389 model) to the spectra-age dataset in Brazil (see Methods). The results showed that there was
390 large variability in leaf $V_{c,max25}$ across leaf life cycles (i.e. from 15-days old to 400-days old), but
391 that the spectroscopy approach presented here was able to track leaf age dependent variation in
392 $V_{c,max25}$ (Fig. 4), particularly during the period from emergence to physiological full-maturity

393 (from 15 to 150 days). With continued aging and senescence (>150 days), there was larger
394 deviation between spectra-predicted and field-observed $V_{c,max25}$. This might largely be because
395 our datasets had poor coverage of older leaves (from 150 days to 400 days), and thus the model
396 for the senescent leaves is not well calibrated.

397

398 Discussion

399 Leaf carboxylation capacity $V_{c,max25}$ is central to the estimation of photosynthetic CO₂
400 uptake by tropical forests in ESMs. In this study, we demonstrated that the spectroscopy
401 approach is able to accurately predict $V_{c,max25}$ across species with a large range in LMA trait
402 space, leaf age, canopy position and height, and forest sites (Fig. 3 and Table S1). We also
403 showed that the combined application of spectroscopy models of leaf $V_{c,max25}$ and age are
404 sufficient to track life time variation in leaf $V_{c,max25}$ (Fig. 4). This represents a significant
405 breakthrough in our ability to rapidly estimate and potentially map $V_{c,max25}$ in high spatial and
406 temporal resolution in tropical forests.

407 Consistent with previous studies (Field, 1983; Sobrado, 1994; Wilson *et al.*, 2001;
408 Kitajima *et al.*, 2002; Kenzo *et al.*, 2006; Pantin *et al.*, 2012; Albert *et al.*, 2018), we found large
409 variability in leaf $V_{c,max25}$ (i.e. 7-102 $\mu\text{mol CO}_2 \text{ m}^{-2} \text{ s}^{-1}$) with species, leaf age and canopy
410 environment across 21 species sampled from the three lowland moist tropical forests. Such a
411 wide range of variability in $V_{c,max25}$ is comparable with previous studies at the same forest sites
412 with larger sample size and a focus on mature leaves (i.e. 15-75 $\mu\text{mol CO}_2 \text{ m}^{-2} \text{ s}^{-1}$ from 65
413 species in Panama, Norby *et al.*, 2017; 10-80 $\mu\text{mol CO}_2 \text{ m}^{-2} \text{ s}^{-1}$ from 38 species in Brazil,
414 Domingues *et al.*, 2014). It is also comparable with the observations from other moist tropical
415 forest sites in Brazil (Carswell *et al.*, 2000), Peru (Bahar *et al.*, 2017) and Africa (Domingues *et*
416 *al.*, 2010).

417 These past studies together with our findings also suggest that leaf age is one of the most
418 important sources of variation in $V_{c,max25}$, which is clearly shown in Figs. 1 and 4. Since $V_{c,max25}$
419 can change markedly with leaf age and our observed $V_{c,max25}$ variability spanned almost the same
420 range (13-90 $\mu\text{mol CO}_2 \text{ m}^{-2} \text{ s}^{-1}$) as that used to represent global variation in $V_{c,max25}$ in current
421 ESMs (Rogers, 2014), it further suggests the importance of including such age-dependent $V_{c,max25}$
422 variation in future model formulations. The high $V_{c,max25}$ variability associated with leaf age also
423 highlights the value of our developed spectroscopy approach to enable rapid estimations of

424 $V_{c,max25}$: the spectroscopy approach only takes a few seconds to estimate $V_{c,max25}$, once the model
425 has been recalibrated, while the conventional approach using leaf gas exchange measurement of
426 a photosynthetic CO_2 response curves takes about an hour (or more). Furthermore, the
427 conventional approach cannot simultaneously derive leaf age—an important piece of information
428 needed to improve model representation of photosynthesis, especially in species-rich, evergreen
429 tropical forests (Kim *et al.*, 2012; Wu *et al.*, 2016).

430 Here we have demonstrated that leaf spectroscopy offers a tool to rapidly capture
431 multiple important axes of variation in $V_{c,max25}$: A single spectra-based model of leaf $V_{c,max25}$ was
432 able to predict leaf $V_{c,max25}$ across tropical tree species with a very large variation in LMA trait
433 space, leaf age, canopy position and forest sites with high confidence (Fig. 3 and Table S1). This
434 finding validates pioneering work that demonstrated not only the feasibility of using leaf spectra
435 to model $V_{c,max}$ under a narrow range of species and conditions (Doughty *et al.*, 2011; Serbin *et*
436 *al.*, 2012), but also dramatically expands our confidence to use the improved spectra- $V_{c,max25}$
437 model across a wide range of species, leaf developmental stages and locations.

438 So what is the underlying mechanism for such a tight covariation between leaf spectra
439 and $V_{c,max25}$ across the various axes of variation (i.e. species, leaf age, canopy positions and forest
440 sites) we considered in this study? There are at least two potential hypotheses.

441 The first is that the tight coordinated variation in leaf $V_{c,max25}$ and spectra was entirely
442 based on their relationships with leaf nitrogen content (e.g. Dechant *et al.*, 2017). The theory
443 underlying this hypothesis is that leaf $V_{c,max25}$ is tightly coupled with the nitrogen content in
444 Rubisco which comprises the largest fraction of N invested in a single enzyme within a leaf (e.g.
445 Jacob *et al.*, 1995; Onoda *et al.*, 2004; Dong *et al.*, 2017; Scafaro *et al.*, 2017; Evans & Clark,
446 2019). This hypothesis seems moderately supported by two previous studies conducted at our
447 study sites (that focused on mature leaves with larger sample size), including significant, but
448 only modest correlations of $V_{c,max25}$ with leaf nitrogen ($R^2=0.31$; Norby *et al.*, 2017; $R^2=0.33$;
449 Dominguez *et al.*, 2014). Given that leaf spectra can efficiently capture variation in leaf nitrogen
450 content (e.g. Asner & Martin, 2008; Serbin *et al.*, 2014; Dechant *et al.*, 2017), it is expected that
451 leaf spectra can also be used to predict leaf $V_{c,max25}$. However, this hypothesis does not stand up
452 to further scrutiny for several reasons. First, if the correlation with leaf nitrogen content was the
453 primary driver of our ability to estimate $V_{c,max25}$ with spectra, it does not explain why leaf spectra
454 shows far higher predictive power than using leaf nitrogen content alone ($R^2=0.89$ for leaf

455 spectra in this study vs. $R^2=0.31-0.33$ for leaf nitrogen content as shown in Dominguez *et al.*,
456 2014 and Norby *et al.*, 2017). Furthermore, the $V_{c,max25}$ -leaf nitrogen relationship does not always
457 hold up at the site level level (Bahar *et al.* 2017; Rogers *et al.*, 2017b; Evans & Clark, 2019) and
458 recent global synthesis have shown that variation in leaf nitrogen can only explain a small
459 portion of variation in $V_{c,max}$ (Ali *et al.*, 2015; Smith *et al.*, 2019). Secondarily, many other
460 studies suggest that in addition to leaf nitrogen content, other leaf traits, e.g. leaf phosphorus
461 content (e.g. Walker *et al.*, 2014; Norby *et al.*, 2017), leaf chlorophyll content (e.g. Croft *et al.*,
462 2017), LMA (e.g. Walker *et al.*, 2014), and age (e.g. Albert *et al.*, 2018), are also related with
463 $V_{c,max25}$, and inclusion of more traits as predictive variables can significantly improve the power
464 of trait based model to predict $V_{c,max25}$, compared with the just one trait, leaf nitrogen content (e.g.
465 Walker *et al.*, 2014). Finally, Serbin *et al.* (2012) showed that in poplar the power of leaf N
466 content and LMA to predict $V_{c,max}$ varied with temperature treatments, but the reflectance
467 spectroscopy approach collapsed this variation into a single model. This suggests that the ability
468 of the spectroscopy approach to predict $V_{c,max}$ is not entirely dependent on the ability of
469 spectroscopy to predict leaf N content and LMA and that other factors are likely contributing to
470 the success of the approach.

471 Since the correlation with leaf nitrogen might not be the only reason for the derived
472 spectra- $V_{c,max25}$ model, this further leads to our second hypothesis: leaf $V_{c,max25}$ is correlated with
473 multiple leaf traits and processes that determine Rubisco content and activity (e.g. leaf nitrogen
474 content, leaf phosphorus content, leaf chlorophyll concentrations, LMA, leaf age, and many
475 others we do not yet understand), and leaf spectra emerge from the ensemble of properties that
476 define leaf chemical, morphological, and phenological status (e.g. Asner & Martin, 2008; Serbin
477 *et al.*, 2014; Chavana-Bryant *et al.*, 2017, 2019). As such, leaf spectra can be used to help infer
478 leaf $V_{c,max25}$, and are indeed a better predictor of leaf $V_{c,max25}$ (e.g. Serbin *et al.*, 2012) than
479 alternative trait approaches that leverage well established links between $V_{c,max25}$ and just one or a
480 few individual leaf traits (e.g. Walker *et al.*, 2014). We believe this second hypothesis offers a
481 more plausible explanation for the power of the spectra- $V_{c,max25}$ approach. However, a more
482 comprehensive study to elucidate the underlying mechanisms that enable the spectra- $V_{c,max25}$
483 model is still needed.

484 Our finding that the spectra- $V_{c,max25}$ model of mature leaves in Panama creates model bias
485 when applied to Panamanian immature leaves and all Brazilian leaves is also interesting. This

486 observation could be attributable to different ranges in $V_{c,max25}$ for model development and
487 validation (e.g. 17-102 $\mu\text{mol CO}_2 \text{ m}^{-2} \text{ s}^{-1}$ for the Panamanian mature leaf model; 21-63 $\mu\text{mol CO}_2$
488 $\text{m}^{-2} \text{ s}^{-1}$ for Panamanian immature leaves; 7-46 $\mu\text{mol CO}_2 \text{ m}^{-2} \text{ s}^{-1}$ for all leaves in Brazil). However,
489 a more likely explanation is that the spectra-trait- $V_{c,max25}$ linkages (e.g. regression coefficients)
490 vary with leaf age (e.g. Field, 1983; Wilson *et al.*, 2001; Chavana-Bryant *et al.*, 2017, 2019; Wu
491 *et al.*, 2017) and forest sites of different soil types and fertility (e.g. Walker *et al.*, 2014; Norby *et*
492 *al.*, 2017). Regardless of these potential reasons, our finding (Fig. 3) suggests that including as
493 many axes of variation as possible in the training dataset is critical to develop a broadly
494 applicable spectra- $V_{c,max25}$ model. Both leaf spectra and $V_{c,max25}$ can vary with vertical canopy
495 profiles (e.g. various canopy positions including upper canopy, mid-canopy and understory trees;
496 sunlit and shaded environments), different tropical forests types (e.g. flooded, Caatinga, second
497 growth, and upland forests) and other leaf habits (e.g. deciduous trees) that are currently either
498 under or not sampled in this study. Therefore we recognize that further in-depth pan-tropical and
499 global sampling and analysis are still needed to develop a highly robust spectra- $V_{c,max25}$ model
500 that can be applied with confidence throughout the tropics and ultimately globally. It is also
501 worth noting that when extending the spectra- $V_{c,max25}$ model to entire vertical canopy profiles, the
502 epiphyll effect is another issue that is needed to be considered, as many old leaves in the shaded
503 canopy environment develop epiphylls (Sonnleitner *et al.*, 2009), which strongly impacts leaf
504 spectral reflectance (see Roberts *et al.*, 1998).

505 We also showed that spectroscopy is able to simulate the life history variability in $V_{c,max25}$
506 with leaf age within and across tropical tree species (Fig. 4). The spectroscopy derived age-
507 dependent $V_{c,max25}$ is also comparable with direct measurements by Wu *et al* (2016) in terms of
508 both amplitude and the relative trend across three leaf developmental stages: young (1-2
509 months), mature (3-5 months) and old (6-14 months). This suggests that the spectroscopy
510 approach can be used to track lifetime trajectories in leaf traits (including but not limited to
511 $V_{c,max25}$ shown here), and is a marked extension of previous studies that demonstrated the
512 feasibility of linking leaf spectroscopy to model leaf $V_{c,max25}$ (e.g. Serbin *et al.*, 2012) or leaf age
513 (e.g. Chavana-Bryant *et al.*, 2017). Moreover, the success of spectroscopy-based $V_{c,max25}$ -age
514 relationships also highlights that the spectroscopy approach can not only be a novel means to
515 capture the variability of $V_{c,max25}$, particularly associated with leaf age, but also rapidly generate
516 datasets that enable the exploration of temporal and spatial variability in $V_{c,max25}$ within and

517 across species, an important piece of process knowledge that greatly needs to be incorporated in
518 future ESMs (e.g. Xu *et al.*, 2017).

519 Finally, our finding that there exists a tight relationship among leaf-level spectra, $V_{c,max25}$
520 and leaf age can likely be extended to canopy and ecosystem scales. As shown by many previous
521 theoretical and empirical studies (Asner, 1998; Asner & Martin, 2008; Ollinger, 2011; Singh *et*
522 *al.*, 2015), the fundamental changes in leaf optical properties with underlying variation in leaf
523 traits is not scale-dependent; that is leaf-level or canopy-scale spectra changes in concert with
524 leaf traits. Meanwhile, Serbin *et al* (2015) demonstrated that the imaging spectroscopy technique
525 could be effectively used to infer leaf $V_{c,max25}$ from canopy-scale hyperspectral reflectance for
526 managed agricultural sites. Given our predictive success at the leaf level, it is possible that our
527 findings could help enable predictions at the canopy level in tropical forest ecosystems.
528 Additionally, Wu *et al* (2018) connected leaf scale optical properties (i.e. reflectance and
529 transmittance) with canopy radiative transfer models to simulate the leaf age effect on canopy
530 reflectance in tropical forest ecosystems. The simulated canopy reflectance from this analysis
531 showed a good agreement with observations from high resolution WorldView-2 imagery, further
532 suggesting a potential way to scale up leaf-scale spectra- $V_{c,max25}$ relationship explored here to the
533 canopy scale. Collectively, these recent studies, together with our current findings (Figs. 3 and
534 4), help build the foundation towards the possibility of monitoring $V_{c,max25}$ -age relationships at
535 canopy and ecosystem scales using state-of-the-art remote sensing technology: e.g. leveraging
536 imaging spectroscopy from unmanned aerial systems (UASs; Adão *et al.*, 2017), aircraft (e.g.
537 AVIRIS, Serbin *et al.*, 2015), and the suite of current and planned space-borne platforms (e.g.
538 EnMAP, Guanter *et al.*, 2015; HISUI, Stavros *et al.*, 2017; Surface Biology and Geology
539 mission, National Academies of Sciences E, Medicine, 2018). Imaging spectroscopy, if
540 successful in capturing $V_{c,max25}$ -age relationships at canopy scales, will greatly advance our
541 capability to monitor and mechanistically understand $V_{c,max25}$ variability across both space and
542 time, providing critically important datasets to parameterize and evaluate ESMs.

543

544

545

546 **Acknowledgements**

547 This work was supported by the Next-Generation Ecosystem Experiments–Tropics project
548 supported by the U.S. DOE, Office of Science, Office of Biological and Environmental Research
549 and through contract #DE-SC0012704 to Brookhaven National Laboratory. L.P.A. was
550 supported by Voss postdoctoral research funding at Brown University. The field work in Brazil
551 was supported by US National Science Foundation (NSF, OISE-0730305). We also acknowledge
552 Mick Eltringham for canopy access assistance in Brazil.

553

554 **Author Contributions**

555 JW, AR, LPA, SRS and SPS designed the study. KE, SPS, AR, BTW and JW collected the field
556 data in Panama. LPA, NP, RCO and JW collected the field data in Brazil. JW performed the data
557 quality control and analysis. JW drafted the manuscript, and all authors contributed to the final
558 version.

559

560 **Competing Interests**

561 The authors declare no competing interests.

562

563

564 **References**

- 565 **Adão T, Hruška J, Pádua L, Bessa J, Peres E, Morais R, Sousa JJ. 2017.** Hyperspectral
566 imaging: A review on UAV-based sensors, data processing and applications for
567 agriculture and forestry. *Remote Sensing* **9**, <https://doi.org/10.3390/rs9111110>.
- 568 **Albert LP, Wu J, Prohaska N, Camargo PB, Huxman TE, Tribuzy ES, Ivanov VY,**
569 **Oliveira RS, Garcia S, Smith MN *et al.* 2018.** Age-dependent leaf physiology and
570 consequences for crown-scale carbon uptake during the dry season in an Amazon
571 evergreen forest. *New Phytologist* **219**: 870-884.
- 572 **Ali AA, Xu C, Rogers A, McDowell NG, Medlyn BE, Fisher RA, Wullschleger SD, Reich**
573 **PB, Vrugt JA, Bauerle WL *et al.* 2015.** Global-scale environmental control of plant
574 photosynthetic capacity. *Ecological Applications* **25**: 2349-2365.
- 575 **Ainsworth EA, Serbin SP, Skoneczka JA, Townsend PA. 2014.** Using leaf optical properties
576 to detect ozone effects on foliar biochemistry. *Photosynthesis Research* **119**: 65-76.
- 577 **Asner GP. 1998.** Biophysical and biochemical sources of variability in canopy
578 reflectance. *Remote Sensing of Environment* **64**: 234-253.
- 579 **Asner GP, Martin RE. 2008.** Spectral and chemical analysis of tropical forests: Scaling from
580 leaf to canopy levels. *Remote Sensing of Environment* **112**: 3958-3970.
- 581 **Asner GP, Martin RE, Tupayachi R, Anderson CB, Sinca F, Carranza-Jiménez L,**
582 **Martinez P. 2014.** Amazonian functional diversity from forest canopy chemical
583 assembly. *Proceedings of the National Academy of Sciences* **111**: 5604-5609.
- 584 **Asner GP, Brodrick PG, Anderson CB, Vaughn N, Knapp DE, Martin RE. 2016.**
585 Progressive forest canopy water loss during the 2012–2015 California
586 drought. *Proceedings of the National Academy of Sciences* **113**: E249-E255.
- 587 **Bahar NH, Ishida FY, Weerasinghe LK, Guerrieri R, O'Sullivan OS, Bloomfield KJ, Asner**
588 **GP, Martin RE, Lloyd J, Malhi Y *et al.* 2017.** Leaf-level photosynthetic capacity in
589 lowland Amazonian and high-elevation Andean tropical moist forests of Peru. *New*
590 *Phytologist* **214**: 1002-1018.
- 591 **Barnes ML, Breshears DD, Law DJ, van Leeuwen WJ, Monson RK, Fojtik AC, Barron-**
592 **Gafford GA, Moore DJ. 2017.** Beyond greenness: Detecting temporal changes in
593 photosynthetic capacity with hyperspectral reflectance data. *PLoS ONE* **12**,
594 <https://doi.org/10.1371/journal.pone.0189539>.

- 595 **Bernacchi CJ, Bagley JE, Serbin SP, RUIZ-VERA UM, Rosenthal DM, Van Loocke A.**
596 **2013.** Modelling C3 photosynthesis from the chloroplast to the ecosystem. *Plant, Cell &*
597 *Environment* **36**: 1641-1657.
- 598 **Bonan GB, Lawrence PJ, Oleson KW, Levis S, Jung M, Reichstein M, Lawrence DM,**
599 **Swenson SC. 2011.** Improving canopy processes in the Community Land Model version
600 4 (CLM4) using global flux fields empirically inferred from FLUXNET data. *Journal of*
601 *Geophysical Research: Biogeosciences* **116**, <https://doi.org/10.1029/2010JG001593>.
- 602 **Carswell FE, Meir P, Wandelli EV, Bonates LCM, Kruijt B, Barbosa EM, Nobre AD,**
603 **Grace J, Jarvis PG. 2000.** Photosynthetic capacity in a central Amazonian rain
604 forest. *Tree Physiology* **20**: 179-186.
- 605 **Chavana-Bryant C, Malhi Y, Wu J, Asner GP, Anastasiou A, Enquist BJ, Caravasi C, Eric**
606 **G, Doughty CE, Saleska SR et al. 2017.** Leaf aging of Amazonian canopy trees as
607 revealed by spectral and physiochemical measurements. *New Phytologist* **214**: 1049-
608 1063.
- 609 **Chavana-Bryant C, Malhi Y, Anastasiou A, Enquist BJ, Cosio EG, Keenan TF, Gerard FF.**
610 **2019.** Leaf age effects on the spectral predictability of leaf traits in Amazonian canopy
611 trees. *Science of the Total Environment* **666**: 1301-1315.
- 612 **Chen S, Hong X, Harris CJ, Sharkey PM. 2004.** Sparse modeling using orthogonal forest
613 regression with PRESS statistic and regularization. *IEEE Transaction on Systems, Man*
614 *and Cybernetics* **34**: 898-911.
- 615 **Coley PD. 1983.** Herbivory and defensive characteristics of tree species in a lowland tropical
616 forest. *Ecological Monographs* **53**: 209-234.
- 617 **Condit RS, Ashton MS, Balslev H, Brokaw NVL, Bunyavejchewin S, Chuyong GB, Co L,**
618 **Dattaraja HS, Davies SJ, Esufali S et al. 2005.** Tropical tree a-diversity: results from a
619 worldwide network of large plots. *Biologiske Skrifter* **55**: 565-582.
- 620 **Croft H, Chen JM, Luo X, Bartlett P, Chen B, Staebler RM. 2017.** Leaf chlorophyll content
621 as a proxy for leaf photosynthetic capacity. *Global Change Biology* **23**: 3513-3524.
- 622 **Curran PJ. 1989.** Remote sensing of foliar chemistry. *Remote Sensing of Environment* **30**: 271-
623 278.

- 624 **Davidson EA, de Araújo AC, Artaxo P, Balch JK, Brown IF, Bustamante MM, Coe MT,**
625 **DeFries RS, Keller M, Longo M *et al.* 2012.** The Amazon basin in
626 transition. *Nature* **481**: 321-328.
- 627 **Dechant B, Cuntz M, Vohland M, Schulz E, Doktor D. 2017.** Estimation of photosynthesis
628 traits from leaf reflectance spectra: correlation to nitrogen content as the dominant
629 mechanism. *Remote Sensing of Environment* **196**: 279-292.
- 630 **De Jong S. 1993.** SIMPLS: an alternative approach to partial least squares
631 regression. *Chemometrics and Intelligent Laboratory Systems* **18**: 251-263.
- 632 **De Kauwe MG, Lin YS, Wright IJ, Medlyn BE, Crous KY, Ellsworth DS, Maire V,**
633 **Prentice IC, Atkin OK, Rogers A *et al.* 2016.** A test of the ‘one-point method’ for
634 estimating maximum carboxylation capacity from field-measured, light-saturated
635 photosynthesis. *New Phytologist* **210**: 1130-1144.
- 636 **De Moura YM, Galvão LS, Hilker T, Wu J, Saleska S, do Amaral CH, Nelson BW, Lopes**
637 **AP, Wiedeman KK, Prohaska N *et al.* 2017.** Spectral analysis of amazon canopy
638 phenology during the dry season using a tower hyperspectral camera and modis
639 observations. *ISPRS Journal of Photogrammetry and Remote Sensing* **131**: 52-64.
- 640 **Díaz S, Kattge J, Cornelissen JH, Wright IJ, Lavorel S, Dray S, Reu B, Kleyer M, Wirth C,**
641 **Prentice IC *et al.* 2016.** The global spectrum of plant form and function. *Nature* **529**:
642 167-171.
- 643 **Domingues TF, Meir P, Feldpausch TR, Saiz G, Veenendaal EM, Schrodte F, Bird M, Hien**
644 **F, Compaore H, Aiallo A *et al.* 2010.** Co-limitation of photosynthetic capacity by
645 nitrogen and phosphorus in West Africa woodlands. *Plant, Cell & Environment* **33**: 959-
646 980.
- 647 **Domingues TF, Martinelli LA, Ehleringer JR. 2014.** Seasonal patterns of leaf-level
648 photosynthetic gas exchange in an eastern Amazonian rain forest. *Plant Ecology &*
649 *Diversity* **7**: 189-203.
- 650 **Dong N, Prentice IC, Evans BJ, Caddy-Retalic S, Lowe AJ, Wright IJ. 2017.** Leaf nitrogen
651 from first principles: field evidence for adaptive variation with climate. *Biogeosciences*
652 **14**: 481–495.
- 653 **Doughty CE, Asner GP, Martin RE. 2011.** Predicting tropical plant physiology from leaf and
654 canopy spectroscopy. *Oecologia* **165**: 289-299.

- 655 **Elvidge CD. 1990.** Visible and near infrared reflectance characteristics of dry plant
656 materials. *International Journal of Remote Sensing* **11**: 1775-1795.
- 657 **Evans JR, Clark VC. 2019.** The nitrogen cost of photosynthesis. *Journal of Experimental*
658 *Botany* **70**: 7-15.
- 659 **Farquhar GV, von Caemmerer SV, Berry JA. 1980.** A biochemical model of photosynthetic
660 CO₂ assimilation in leaves of C3 species. *Planta* **149**: 78-90.
- 661 **Field C. 1983.** Allocating leaf nitrogen for the maximization of carbon gain: leaf age as a control
662 on the allocation program. *Oecologia* **56**: 341-347.
- 663 **Geladi P, Kowalski BR. 1986.** Partial least-squares regression: a tutorial. *Analytica Chimica*
664 *Acta* **185**: 1-17.
- 665 **Guanter L, Kaufmann H, Segl K, Foerster S, Rogass C, Chabrillat S, Kuester T, Hollstein**
666 **A, Rossner G, Chlebek C, et al. 2015.** The EnMAP spaceborne imaging spectroscopy
667 mission for earth observation. *Remote Sensing* **7**: 8830-8857.
- 668 **Han Q, Kawasaki T, Nakano T, Chiba Y. 2008.** Leaf-age effects on seasonal variability in
669 photosynthetic parameters and its relationships with leaf mass per area and leaf nitrogen
670 concentration within a *Pinus densiflora* crown. *Tree Physiology* **28**: 551-558.
- 671 **Hutyra LR, Munger JW, Saleska SR, Gottlieb E, Daube BC, Dunn AL, Amaral DF, de**
672 **Camargo PB, Wofsy SC. 2007.** Seasonal controls on the exchange of carbon and water
673 in an Amazonian rain forest. *Journal of Geophysical Research: Biogeosciences* **112**:
674 G03008, <https://doi.org/10.1029/2006JG000365>.
- 675 **Jacob J, Greitner C, Drake BG. 1995.** Acclimation of photosynthesis in relation to Rubisco
676 and non-structural carbohydrate contents and in situ carboxylase activity in *Scirpus*
677 *olneyi* grown at elevated CO₂ in the field. *Plant, Cell & Environment* **18**: 875-884.
- 678 **Kattge J, Knorr W. 2007.** Temperature acclimation in a biochemical model of photosynthesis: a
679 reanalysis of data from 36 species. *Plant, Cell & Environment* **30**: 1176-1190.
- 680 **Kattge J, Diaz S, Lavorel S, Prentice IC, Leadley P, Bönisch G, Garnier E, Westoby M,**
681 **Reich PB, Wright IJ et al. 2011.** TRY—a global database of plant traits. *Global Change*
682 *Biology* **17**: 2905-2935.
- 683 **Kenzo T, Ichie T, Watanabe Y, Yoneda R, Ninomiya I, Koike T. 2006.** Changes in
684 photosynthesis and leaf characteristics with tree height in five dipterocarp species in a
685 tropical rain forest. *Tree Physiology* **26**: 865-873.

- 686 **Kim Y, Knox RG, Longo M, Medvigy D, Hutyra LR, Pyle EH, Wofsy SC, Bras RL,**
687 **Moorcroft, PR. 2012.** Seasonal carbon dynamics and water fluxes in an Amazon
688 rainforest. *Global Change Biology* **18**: 1322-1334.
- 689 **Kitajima K, Mulkey SS, Samaniego M, Wright J.S. 2002.** Decline of photosynthetic capacity
690 with leaf age and position in two tropical pioneer tree species. *American Journal of*
691 *Botany* **89**: 1925-1932.
- 692 **Kokaly RF, Asner GP, Ollinger SV, Martin ME, Wessman CA. 2009.** Characterizing canopy
693 biochemistry from imaging spectroscopy and its application to ecosystem studies. *Remote*
694 *Sensing of Environment* **113**: S78-S91.
- 695 **Kumarathunge DP, Medlyn BE, Drake JE, Tjoelker MG, Aspinwall MJ, Battaglia M,**
696 **Cano FJ, Carter KR, Cavaleri MA, Cernusak LA, Chamber JQ, Crous KY et al.**
697 **2019.** Acclimation and adaptation components of the temperature dependence of plant
698 photosynthesis at the global scale. *New Phytologist* **222**: 768-784.
- 699 **Long SP, Bernacchi CJ. 2003.** Gas exchange measurements, what can they tell us about the
700 underlying limitations to photosynthesis? Procedures and sources of error. *Journal of*
701 *Experimental Botany* **54**: 2393-2401.
- 702 **Lopes AP, Nelson BW, Wu J, de Alencastro GPML, Tavares JV, Prohaska N, Martins GA,**
703 **Saleska SR. 2016.** Leaf flush drives dry season green-up of the central Amazon. *Remote*
704 *Sensing of Environment* **182**: 90-98.
- 705 **Medlyn BE, Badeck FW, De Pury DGG, Barton CVM, Broadmeadow M, Ceulemans R, De**
706 **Angelis P, Forstreuter M, Jach ME, Kellomäki S et al. 1999.** Effects of elevated [CO₂]
707 on photosynthesis in European forest species: a meta-analysis of model
708 parameters. *Plant, Cell & Environment* **22**: 1475-1495.
- 709 **Muraoka H, Saigusa N, Nasahara KN, Noda H, Yoshino J, Saitoh TM, Nagai S, Murayama**
710 **S, Koizumi H. 2010.** Effects of seasonal and interannual variations in leaf photosynthesis
711 and canopy leaf area index on gross primary production of a cool-temperate deciduous
712 broadleaf forest in Takayama, Japan. *Journal of Plant Research* **123**: 563-576.
- 713 **National Academies of Sciences E, Medicine. 2018.** *Thriving on Our Changing Planet: A*
714 *Decadal Strategy for Earth Observation from Space*. Washington, DC: The National
715 Academies Press.

- 716 **Nepstad DC, Moutinho P, Dias-Filho MB, Davidson E, Cardinot G, Markewitz D,**
717 **Figueiredo R, Vianna N, Chambers J, Ray D *et al.* 2002.** The effects of partial
718 throughfall exclusion on canopy processes, aboveground production, and
719 biogeochemistry of an Amazon forest. *Journal of Geophysical Research:*
720 *Atmospheres* **107**: <https://doi.org/10.1029/2001JD000360>.
- 721 **Niinemets, U. 2016.** Leaf age dependent changes in within-canopy variation in leaf functional
722 traits: a meta-analysis. *Journal of Plant Research* **129**: 313–338.
- 723 **Norby RJ, Gu L, Haworth IC, Jensen AM, Turner BL, Walker AP, Warren JM, Weston**
724 **DJ, Xu C, Winter K. 2017.** Informing models through empirical relationships between
725 foliar phosphorus, nitrogen and photosynthesis across diverse woody species in tropical
726 forests of Panama. *New Phytologist* **215**: 1425-1437.
- 727 **Ollinger SV. 2011.** Sources of variability in canopy reflectance and the convergent properties of
728 plants. *New Phytologist* **189**: 375-394.
- 729 **Onoda Y, Hikosaka K, Hirose T. 2004.** Seasonal change in the balance between capacities of
730 RuBP carboxylation and RuBP regeneration affects CO₂ response of photosynthesis in
731 *Polygonum cuspidatum*. *Journal of Experimental Botany* **56**: 755-763.
- 732 **Pantin F, Simonneau T, Muller B. 2012.** Coming of leaf age: control of growth by hydraulics
733 and metabolics during leaf ontogeny. *New Phytologist* **196**: 349-366.
- 734 **Reich PB, Uhl C, Walters MB, Prugh L, Ellsworth DS. 2004.** Leaf demography and
735 phenology in Amazonian rain forest: a census of 40000 leaves of 23 tree
736 species. *Ecological Monographs* **74**: 3-23.
- 737 **Ricciuto D, Sargsyan K, Thornton P. 2018.** The impact of parametric uncertainties on
738 biogeochemistry in the E3SM land model. *Journal of Advances in Modeling Earth*
739 *Systems* **10**: 297-319.
- 740 **Rice AH, Pyle EH, Saleska SR, Hutrya L, Palace M, Keller M, De Camargo PB, Portilho K,**
741 **Marques DF, Wofsy SC. 2004.** Carbon balance and vegetation dynamics in an
742 old-growth Amazonian forest. *Ecological Applications* **14**: 55-71.
- 743 **Roberts DA, Nelson BW, Adams JB, Palmer F. 1998.** Spectral changes with leaf aging in
744 Amazon caatinga. *Trees* **12**: 315-325.
- 745 **Rogers A. 2014.** The use and misuse of V_{c,max} in Earth System Models. *Photosynthesis*
746 *Research* **119**: 15-29.

- 747 **Rogers A, Medlyn BE, Dukes JS, Bonan G, Caemmerer S, Dietze MC, Kattge J, Leakey**
748 **AD, Mercado LM, Niinemets Ü *et al.* 2017a.** A roadmap for improving the
749 representation of photosynthesis in Earth system models. *New Phytologist* **213**: 22-42.
- 750 **Rogers A, Serbin SP, Ely KS, Sloan VL, Wullschleger SD. 2017b.** Terrestrial biosphere
751 models underestimate photosynthetic capacity and CO₂ assimilation in the Arctic. *New*
752 *Phytologist* **216**: 1090-1103.
- 753 **Rosipal R, Krämer N. 2006.** Overview and recent advances in partial least squares.
754 In Saunders, C., Grobelink, M., Gunn, S., & Shawe-Taylor, J. (Eds.), *Subspace, Latent*
755 *Structure and Feature Selection*. Berlin: Springer, 34-51.
- 756 **Scafaro AP, Xiang S, Long BM, Bahar NH, Weerasinghe LK, Creek D, Evans JR, Reich**
757 **PB, Atkin OK. 2017.** Strong thermal acclimation of photosynthesis in tropical and
758 temperate wet-forest tree species: the importance of altered Rubisco content. *Global*
759 *Change Biology* **23**: 2783-2800.
- 760 **Schimel D, Pavlick R, Fisher JB, Asner GP, Saatchi S, Townsend P, Miller C, Frankenberg**
761 **C, Hibbard K, Cox P. 2015.** Observing terrestrial ecosystems and the carbon cycle from
762 space. *Global Change Biology* **21**: 1762-1776.
- 763 **Schneider FD, Morsdorf F, Schmid B, Petchey OL, Hueni A, Schimel DS, Schaepman ME.**
764 **2017.** Mapping functional diversity from remotely sensed morphological and
765 physiological forest traits. *Nature Communications* **8**: 1441-1441,
766 <https://doi.org/10.1038/s41467-017-01530-3>.
- 767 **Schweiger AK, Cavender-Bares J, Townsend PA, Hobbie SE, Madritch MD, Wang R,**
768 **Tilman D, Gamon J A. 2018.** Plant spectral diversity integrates functional and
769 phylogenetic components of biodiversity and predicts ecosystem function. *Nature*
770 *Ecology & Evolution* **2**: 976-982.
- 771 **Serbin SP, Dillaway DN, Kruger EL, Townsend PA. 2012.** Leaf optical properties reflect
772 variation in photosynthetic metabolism and its sensitivity to temperature. *Journal of*
773 *Experimental Botany* **63**: 489-502.
- 774 **Serbin SP, Singh A, McNeil BE, Kingdon CC, Townsend PA. 2014.** Spectroscopic
775 determination of leaf morphological and biochemical traits for northern temperate and
776 boreal tree species. *Ecological Applications* **24**: 1651-1669.

- 777 **Serbin SP, Singh A, Desai AR, Dubois SG, Jablonski AD, Kingdon CC, Kruger EL,**
778 **Townsend PA. 2015.** Remotely estimating photosynthetic capacity, and its response to
779 temperature, in vegetation canopies using imaging spectroscopy. *Remote Sensing of*
780 *Environment* **167**: 78-87.
- 781 **Sharkey TD, Bernacchi CJ, Farquhar GD, Singaas EL. 2007.** Fitting photosynthetic carbon
782 dioxide response curves for C3 leaves. *Plant, Cell & Environment* **30**: 1035-1040.
- 783 **Silva-Perez V, Molero G, Serbin SP, Condon AG, Reynolds MP, Furbank RT, Evans JR.**
784 **2018.** Hyperspectral reflectance as a tool to measure biochemical and physiological traits
785 in wheat. *Journal of Experimental Botany* **3**: 483-496.
- 786 **Singh A, Serbin SP, McNeil BE, Kingdon CC, Townsend PA. 2015.** Imaging spectroscopy
787 algorithms for mapping canopy foliar chemical and morphological traits and their
788 uncertainties. *Ecological Applications* **25**: 2180-2197.
- 789 **Smith NJ, Keenan TF, Prentice IC, Wang H, Wright IJ, Niinemets U, Crous KY,**
790 **Domingues TF, Guerrieri R, Ishida FY et al. 2019.** Global photosynthetic capacity is
791 optimized to the environment. *Ecology Letters* **22**: 506-517.
- 792 **Sobrado MA. 1994.** Leaf age effects on photosynthetic rate, transpiration rate and nitrogen
793 content in a tropical dry forest. *Physiologia Plantarum* **90**: 210-215.
- 794 **Sonnleitner M, Dullinger S, Wanek W, Zechmeister H. 2009.** Microclimatic patterns correlate
795 with the distribution of epiphyllous bryophytes in a tropical lowland rain forest in Costa
796 Rica. *Journal of Tropical Ecology* **25**: 321-330.
- 797 **Sperry J. 2013.** Cutting-edge research or cutting-edge artefact? An overdue control experiment
798 complicates the xylem refilling story. *Plant, Cell & Environment* **36**: 1916-1918.
- 799 **Stavros EN, Schimel D, Pavlick R, Serbin S, Swann A, Duncanson L, Fisher JB, Fassnacht**
800 **F, Ustin S, Dubayah R et al. 2017.** ISS observations offer insights into plant
801 function. *Nature Ecology and Evolution* **1**: 0194.
- 802 **Steege H, Pitman NC, Sabatier D, Baraloto C, Salomão RP, Guevara JE, Phillips OL,**
803 **Castilho CV, Magnusson WE, Molino JF et al. 2013.** Hyperdominance in the
804 Amazonian tree flora. *Science* **342**: 1243092.
- 805 **Stinziano JR, Morgan PB, Lynch DJ, Saathoff AJ, McDermitt DK, Hanson DT. 2017.** The
806 rapid A–Ci response: photosynthesis in the phenomic era. *Plant, Cell & Environment* **40**:
807 1256-1262.

- 808 **Turner BL, Romero TE. 2009.** Short-term changes in extractable inorganic nutrients during
809 storage of tropical rain forest soils. *Soil Science Society of America Journal* **73**: 1972-
810 1979.
- 811 **Walker AP, Beckerman AP, Gu L, Kattge J, Cernusak LA, Domingues TF, Scales JC,**
812 **Wohlfahrt G, Wullschleger SD, Woodward FI. 2014.** The relationship of leaf
813 photosynthetic traits— V_{cmax} and J_{max} —to leaf nitrogen, leaf phosphorus, and specific leaf
814 area: a meta-analysis and modeling study. *Ecology and Evolution* **4**: 3218-3235.
- 815 **Walker AP, Quaipe T, Bodegom PM, De Kauwe MG, Keenan TF, Joiner J, Lomas MR,**
816 **MacBean N, Xu C, Yang X et al. 2017.** The impact of alternative trait-scaling
817 hypotheses for the maximum photosynthetic carboxylation rate (V_{cmax}) on global gross
818 primary production. *New Phytologist* **215**: 1370-1386.
- 819 **Wilson KB, Baldocchi DD, Hanson PJ. 2001.** Leaf age affects the seasonal pattern of
820 photosynthetic capacity and net ecosystem exchange of carbon in a deciduous
821 forest. *Plant, Cell & Environment* **24**: 571-583.
- 822 **Wolter PT, Townsend PA, Sturtevant BR, Kingdon CC. 2008.** Remote sensing of the
823 distribution and abundance of host species for spruce budworm in Northern Minnesota
824 and Ontario. *Remote Sensing of Environment* **112**: 3971-3982.
- 825 **Wright SJ, Horlyck V, Basset Y, Barrios H, Bethancourt A, Bohlman SA, Gilbert GS,**
826 **Goldstein G, Graham EA, Kitajima K et al. 2003.** Tropical canopy biology program,
827 Republic of Panama. *Studying forest canopies from above: the International Canopy*
828 *Crane Network*, eds Basset, Y., Horlyck, V., & Wright, S.J. (Smithsonian Tropical
829 Research Institute and the United Nations Environmental Programme, Panama City,
830 Panama), 137-155.
- 831 **Wu J, Albert LP, Lopes AP, Restrepo-Coupe N, Hayek M, Wiedemann KT, Guan K, Stark**
832 **SC, Christoffersen B, Prohaska N et al. 2016.** Leaf development and demography
833 explain photosynthetic seasonality in Amazon evergreen forests. *Science* **351**: 972-976.
- 834 **Wu J, Chavana-Bryant C, Prohaska N, Serbin SP, Guan K, Albert LP, Yang X, Leeuwen**
835 **WJ, Garnello AJ, Martins G et al. 2017.** Convergence in relationships between leaf
836 traits, spectra and age across diverse canopy environments and two contrasting tropical
837 forests. *New Phytologist* **214**: 1033-1048.

- 838 **Wu J, Kobayashi H, Stark SC, Meng R, Guan K, Tran NN, Gao S, Yang W,**
839 **Restrepo-Coupe N, Miura T *et al.* 2018.** Biological processes dominate seasonality of
840 remotely sensed canopy greenness in an Amazon evergreen forest. *New Phytologist* **217:**
841 1507-1520.
- 842 **Xu QS, Liang YZ. 2001.** Monte Carlo cross validation. *Chemometrics and Intelligent*
843 *Laboratory Systems* **56:** 1-11.
- 844 **Xu X, Medvigy D, Wright JS, Kitajima K, Wu J, Albert LP, Martins GA, Saleska SR,**
845 **Pacala SW. 2017.** Variations of leaf longevity in tropical moist forests predicted by a
846 trait-driven carbon optimality model. *Ecology Letters* **20:** 1097-1106.
- 847 **Yendrek C, Tomaz T, Montes CM, Cao Y, Morse AM, Brown PJ, McIntyre L, Leakey A,**
848 **Ainsworth E. 2017.** High-throughput phenotyping of maize leaf physiology and
849 biochemistry using hyperspectral reflectance. *Plant Physiology* **173:** 614-626.
850

851 **Figure legends**

852 **Figure 1.** Large variation in leaf $V_{c,max25}$ (a) within individual trees and (b) across tropical
853 forests. The data were from the Tapajos K67 site in Brazil, the San Lorenzo crane site (SLZ) and
854 the Parque Natural Metropolitano crane site (PNM) in The Republic of Panama. At the
855 individual tree level (panel a), $V_{c,max25}$ is primarily associated with leaf development (orange for
856 variation in mature leaves, and blue for variation in immature leaves; see Methods) and canopy
857 position (circles for the leaves sampled from the sunlit canopy environment, and triangles for the
858 leaves sampled from the shaded canopy environment). Across tropical forests (panel b), the
859 spread of tree specific (sunlit canopy, mature leaves) mean $V_{c,max25}$ of each forest site is displayed
860 with a boxplot, in which the central mark is the median, the edges are the 25th and 75th
861 percentiles, and the whiskers are the 5th and 95th percentiles.

862 **Figure 2.** A spectra- $V_{c,max25}$ model was trained using two thirds of the dataset from mature leaves
863 measured in Panama, and then evaluated using the independent validation dataset collected in (a)
864 Panamanian mature leaves, (b) Panamanian immature leaves, (c) Brazilian mature and immature
865 leaves, and (d) all leaf classes collected in Panama and Brazil. Error bars denote the 95%
866 confidence intervals for each predicted value based on the ensemble PLSR models (i.e. each
867 PLSR model is represented by a set of PLSR fitted spectral coefficients, and in total includes 100
868 Monte-Carol model runs; see Methods); the gray line shows the ordinary least square regression
869 fit, and the black line shows the 1:1 line.

870 **Figure 3.** The final spectra- $V_{c,max25}$ model was trained using two thirds of our entire dataset, and
871 then applied to the remaining, independent validation dataset. Error bars denote the 95%
872 confidence intervals for each predicted value based on the ensemble PLSR models, the gray line
873 shows the ordinary least square regression fit, and the black line shows the 1:1 line.

874 **Figure 4.** The combination of our final spectral model for $V_{c,max25}$ (Fig. 3) and the leaf age model
875 (see Wu *et al.*, 2017; also see Methods) enables the prediction of the life history trajectories of
876 leaf $V_{c,max25}$ (grey circles) in an independent spectra-age dataset collected in Brazil (see
877 Methods). Here we show that for a given leaf age (determined by the spectra model) we can
878 capture the dynamics of field observed $V_{c,max25}$ (red circles). See Table S1 for the full species
879 names, error bars denote the 95% confidence interval of spectral predictions.

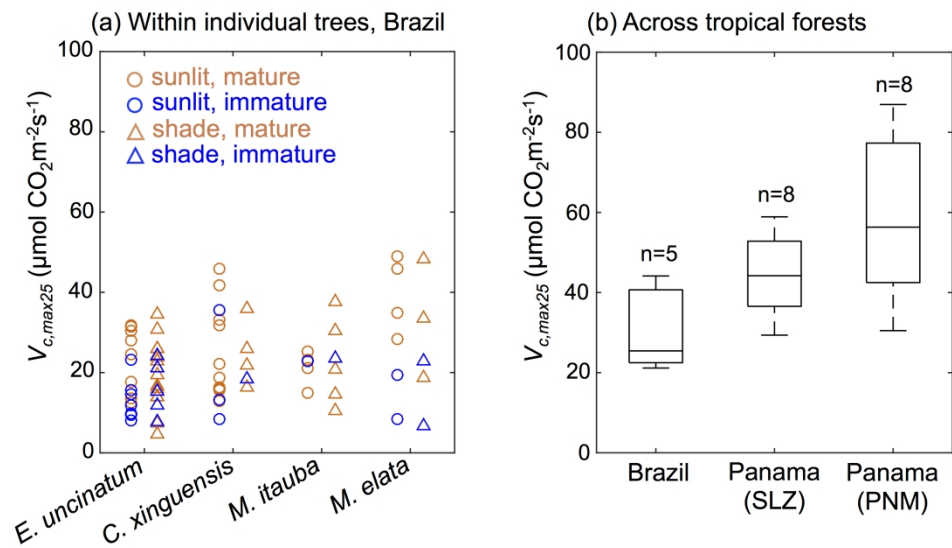


Figure 1. Large variation in leaf $V_{c,max25}$ (a) within individual trees and (b) across tropical forests. The data were from the Tapajos K67 site in Brazil, the San Lorenzo crane site (SLZ) and the Parque Natural Metropolitano crane site (PNM) in The Republic of Panama. At the individual tree level (panel a), $V_{c,max25}$ is primarily associated with leaf development (orange for variation in mature leaves, and blue for variation in immature leaves; see Methods) and canopy position (circles for the leaves sampled from the sunlit canopy environment, and triangles for the leaves sampled from the shaded canopy environment). Across tropical forests (panel b), the spread of tree specific (sunlit canopy, mature leaves) mean $V_{c,max25}$ of each forest site is displayed with a boxplot, in which the central mark is the median, the edges are the 25th and 75th percentiles, and the whiskers are the 5th and 95th percentiles.

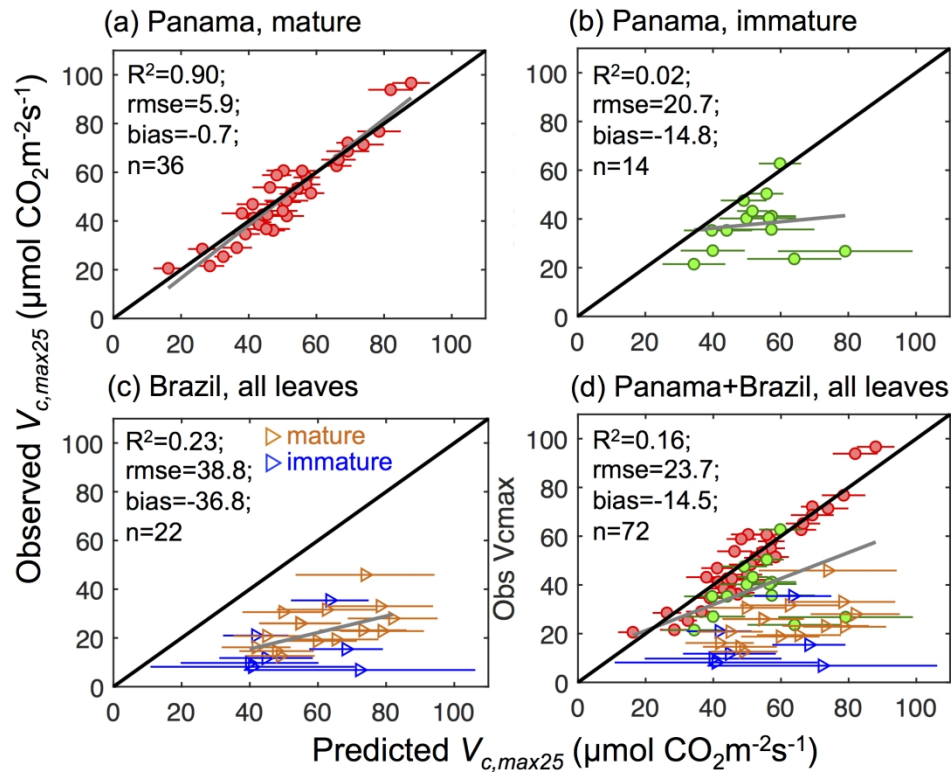


Figure 2. A spectra- $V_{c,max25}$ model was trained using two thirds of the dataset from mature leaves measured in Panama, and then evaluated using the independent validation dataset collected in (a) Panamanian mature leaves, (b) Panamanian immature leaves, (c) Brazilian mature and immature leaves, and (d) all leaf classes collected in Panama and Brazil. Error bars denote the 95% confidence intervals for each predicted value based on the ensemble PLSR models (i.e. each PLSR model is represented by a set of PLSR fitted spectral coefficients, and in total includes 100 Monte-Carlo model runs; see Methods); the gray line shows the ordinary least square regression fit, and the black line shows the 1:1 line.

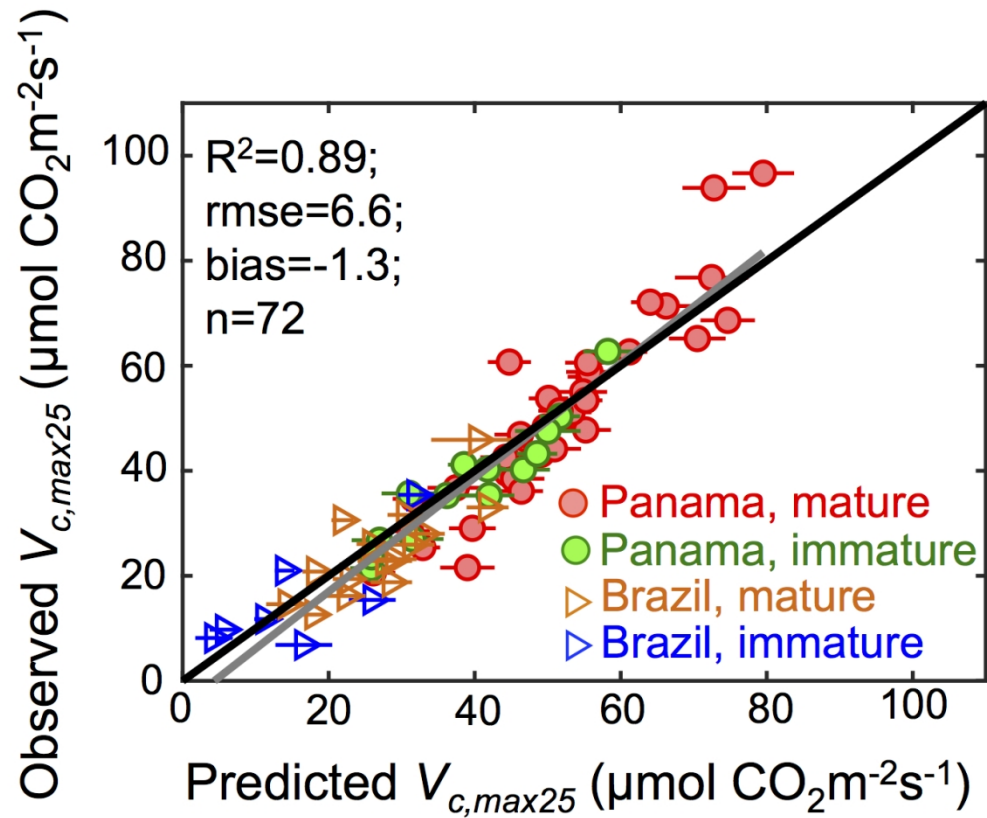


Figure 3. The final spectra- $V_{c,max25}$ model was trained using two thirds of our entire dataset, and then applied to the remaining, independent validation dataset. Error bars denote the 95% confidence intervals for each predicted value based on the ensemble PLSR models, the gray line shows the ordinary least square regression fit, and the black line shows the 1:1 line.

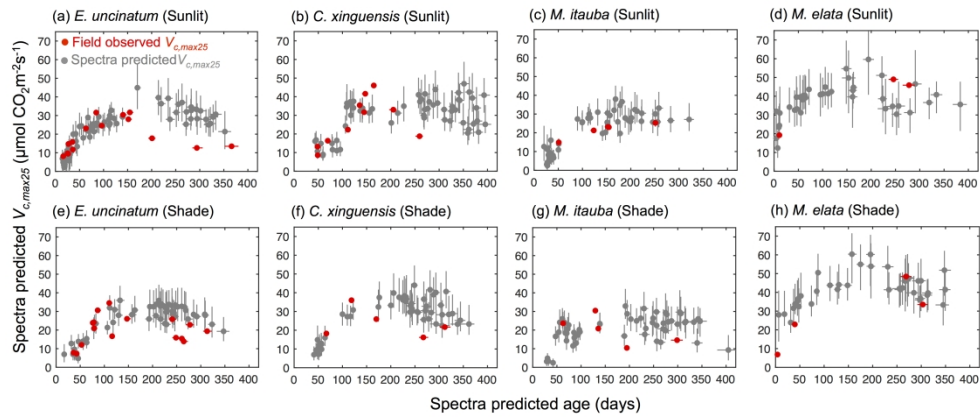


Figure 4. The combination of our final spectral model for $V_{c,max25}$ (Fig. 3) and the leaf age model (see Wu et al., 2017; also see Methods) enables the prediction of the life history trajectories of leaf $V_{c,max25}$ (grey circles) in an independent spectra-age dataset collected in Brazil (see Methods). Here we show that for a given leaf age (determined by the spectra model) we can capture the dynamics of field observed $V_{c,max25}$ (red circles). See Table S1 for the full species names, error bars denote the 95% confidence interval of spectral predictions.